Development of Ectopic Livers by Hepatocyte Transplantation Into Swine Lymph Nodes

Paulo Fontes,[1,2]* Junji Komori,[3,4]* Roberto Lopez,[1,2] Wallis Marsh,[1] and Eric Lagasse[2,3]

[1]WVU Medicine, Department of Surgery, School of Medicine, West Virginia University, Morgantown, WV; [2]LyGenesis, Inc., Pittsburgh, PA; [3]McGowan Institute for Regenerative Medicine, Department of Pathology, School of Medicine, University of Pittsburgh, Pittsburgh, PA; and [4]Department of Surgery, Takamatsu Red Cross Hospital, Kagawa, Japan

Orthotopic liver transplantation continues to be the only effective therapy for patients with end-stage liver disease. Unfortunately, many of these patients are not considered transplant candidates, lacking effective therapeutic options that would address both the irreversible progression of their hepatic failure and the control of their portal hypertension. In this prospective study, a swine model was exploited to induce subacute liver failure. Autologous hepatocytes, isolated from the left hepatic lobe, were transplanted into the mesenteric lymph nodes (LNs) by direct cell injection. At 30-60 days after transplantation, hepatocyte engraftment in LNs was successfully identified in all transplanted animals with the degree of ectopic liver mass detected being proportional to the induced native liver injury. These ectopic livers developed within the LNs showed remarkable histologic features of swine hepatic lobules, including the formation of sinusoids and bile ducts. On the basis of our previous tyrosinemic mouse model and the present pig models of induced subacute liver failure, the generation of auxiliary liver tissue using the LNs as hepatocyte engraftment sites represents a potential therapeutic approach to supplement declining hepatic function in the treatment of liver disease.

Liver Transplantation 26 1629–1643 2020 AASLD.
Received May 25, 2020; accepted August 9, 2020.

Liver diseases are responsible for over 30,000 deaths annually in the United States.[1] Orthotopic liver transplantation (OLT) is too often the last resort and, currently, the only curative treatment for patients suffering from irreversible hepatic failure.[2,3] Yet, OLT remains limited to the patients with favorable clinical conditions that would allow them to undergo a major operative procedure. Up to 30% of the patients with end-stage liver disease (ESLD) requiring OLT are either not considered candidates due to significant comorbidities and advanced age or are expected to have reduced posttransplant survival.[4-6] Furthermore, donor shortage remains a major challenge facing potential organ recipients affected by ESLD. Lastly, the cost of these operative procedures is an additional concern. For these reasons, cell-based transplantation has been proposed as one therapeutic alternative to OLT or as a bridge therapy while patients are waiting for organ transplantation.[7]

To date, hepatocyte transplantation has demonstrated its functional utility in some limited animal models. From the transgenic urokinase[8-10] to the induced tyrosinemic mouse and pig models,[11-19] hepatocyte transplantation has successfully established its therapeutic potential with complete regeneration of the liver. Despite this encouraging prospect, human hepatocyte transplantation is still an experimental

Abbreviations: α-SMA, α smooth muscle actin; ABCB1, ATP binding cassette B1; ABCC2, ATP binding cassette C2; ACTB, β-actin; ALB, albumin; ALP, alkaline phosphatase; ALT, alanine aminotransferase; ASGR1, asialoglycoprotein receptor 1; AST, aspartate aminotransferase; BSA, bovine serum albumin; BSEP, bile salt export pump; CK, cytokeratin; CYP27A1, cytochrome P450 27A1; CYP7A1, cytochrome P450 7A1; DPP4, dipeptidyl peptidase–4; ELISA, enzyme-linked immunosorbent assay; EpCAM, epithelial cell adhesion molecule; ESLD, end-stage liver disease; GGT, gamma-glutamyl transpeptidase; H & E, hematoxylin-eosin; HE, hepatic encephalopathy; IV, intravenous; IVC, inferior vena cava; LLH, left lateral lobe hepatectomy; LLS, left lateral segment; LN, lymph node; LYVE1, lymphatic vessel endothelial hyaluronan receptor 1; mRNA, messenger RNA; MRP2, multidrug resistance–associated protein 2; OLT, orthotopic liver transplantation; OR, operative room; OTC, ornithine carbamoyltransferase; PBS, phosphate-buffered saline; PCR, polymerase chain reaction; PCS, portacaval shunt; PFA, paraformaldehyde; PNAd, peripheral node addressin; po, per os; PPIA, peptidylprolyl isomerase A; PV, portal vein; RPVL, right portal vein ligation; SD, standard deviation; SMV, superior mesenteric vein; TBA, total bile acid.

procedure[7,20] with the expectation that successful preclinical animal studies would be further translated into innovative clinical options. For patients with ESLD, there is an additional challenge: most cellular therapies require cell engraftment in the diseased liver. Transplanted hepatocytes are generally injected in the spleen through the splenic artery, directly into the splenic parenchyma, or intravenously into the liver, through the portal vein (PV). Injected hepatocytes can rapidly migrate, actively or passively, to the diseased liver, regenerating hepatic mass. Such an approach limits, and possibly prevents, the efficacy of cellular therapy in a vast majority of patients with ESLD due to the presence of poor vascularized tissue in their diseased fibrotic and cirrhotic livers.[21] Furthermore, portal hypertension is a major complication of ESLD, making hepatocyte transplantation into a high-pressure portal system a risky procedure. In ESLD patients with massive fibrosis and irreversible lobular disarray, the intended induction of native liver regeneration by cell transplantation is a major biological challenge, and alternative sites for hepatocyte transplantation should be considered to meet the continued and substantial clinical demand while providing potential therapeutic benefits through meaningful cell engraftment.

Previously, our laboratory showed that primary hepatocytes transplanted into tyrosinemic mice jejunal lymph node (LN) will engraft, proliferate, and generate an ectopic liver that will rescue the animal from a fatal liver disease. Here, as a first step to address the lack of an effective therapeutic option that would affect both the control of portal hypertension and the subsequent enhancement of the total functional hepatocellular mass, we developed a protocol in an outbred pig model to surgically induce subacute hepatic failure. The aim of this study was to evaluate safety and feasibility of hepatocyte transplantation into LNs and to generate an ectopic liver tissue in a large animal model of subacute hepatic failure, different from the mouse tyrosinemic model.

Address reprint requests to Eric Lagasse, Pharm.D., Ph.D., McGowan Institute for Regenerative Medicine, Department of Pathology, School of Medicine, University of Pittsburgh, 450 Technology Drive, Room 329, Pittsburgh, PA 15219. Telephone: 412-624 5285; FAX: 412-624-5363; E-mail: lagasse@pitt.edu

Eric Lagasse is the Chief Science Officer, Paulo Fontes is the Chief Medical Officer, and Roberto Lopez is a consultant to LyGenesis, Inc., and all own shares in the company.

This study was supported by an intramural research grant from the McGowan Institute for Regenerative Medicine and the National Institutes of Health, National Institute of Diabetes and Digestive and Kidney Diseases (R01DK114282 to Eric Lagasse).

**These authors contributed equally to this work.*

View this article online at wileyonlinelibrary.com.

DOI 10.1002/lt.25872

Materials and Methods

ANIMALS

Six-month-old female Landrace pigs (~70 kg) from a certified vendor (Animal Biotech Industries, Inc., Doylestown, PA) were used in this study. All animal procedures were performed in compliance with the University of Pittsburgh after the approval of a protocol by the Institutional Animal Care and Use Committee regulations and were conducted within US Department of Agriculture regulations and an Association for Assessment and Accreditation of Laboratory Animal Care International facility.

SWINE MODELS OF LIVER INJURY

The swine models of liver injury were conceived as the translational proof-of-concept preclinical experiments based on our encouraging results obtained with a *fah*$^{-/-}$ mouse model of tyrosinemia type 1.[22,23] We applied a similar concept in this Landrace swine model, where a surgically induced liver injury (right portal vein ligation [RPVL] or portacaval shunt [PCS]) with partial hepatectomy was followed by hepatocyte transplantation into the mesenteric and perihepatic LNs. All animals included in this study were transplanted as described in the schematic illustration of Fig. 1A. The purpose of autologous hepatocyte transplantation was to minimize immunogenicity while avoiding issues related to the use of immunosuppressive therapy.

EXPERIMENTAL DESIGN

The operative procedures were conducted by a team of senior transplant and hepatobiliary surgeons and under general anesthesia provided by certified animal

A

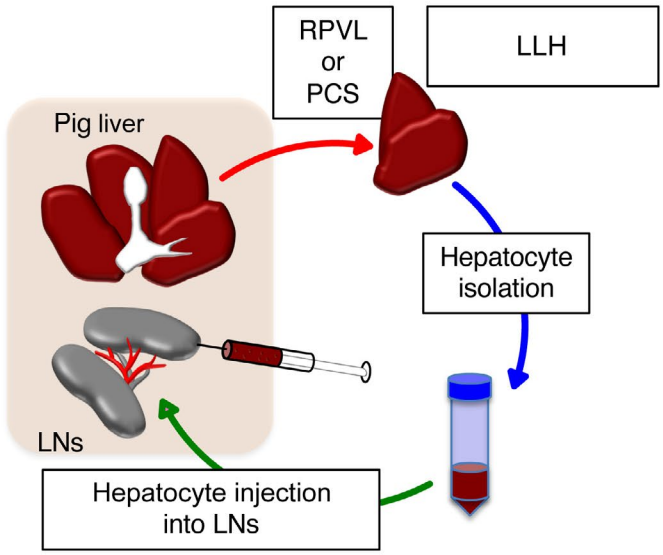

B

Animal Identification Number	Liver Injury*	Number of Cells Transplanted†	Number of LNs Transplanted	Days After Transplant
P35-12	RPVL	360	3	30
P36-12	RPVL	750	9	30
P37-12	RPVL	1250	11	30
P148-12	PCS	1270	13	30
P194-12	PCS	1376	16	60
P147-13	PCS	1862	18	60

*RPVL or PCS in addition to the LLH.
†Number of hepatocytes transplanted (in millions).

C

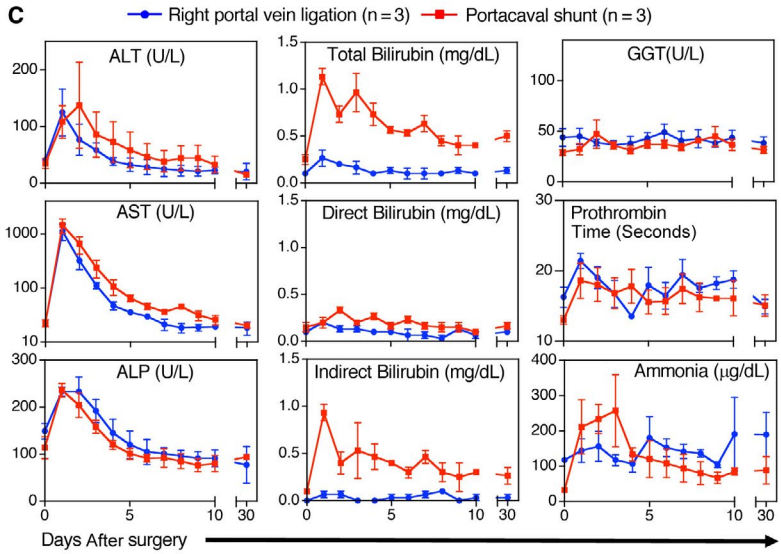

FIG. 1. Ectopic transplantation of hepatocytes in swine models of subacute hepatic failure. (A) Schematic representation of the procedure. (B) Summary table of hepatocyte transplantations in 2 surgically induced liver injury models (RPVL or PCS). The number of cells injected and the number of LNs transplanted is shown. (C) Biochemical parameters during the course of the experiments (30 days). Results are expressed as mean ± SD of biochemical markers in animals with RPVL plus left lobe hepatectomy (n = 3, blue line) or complete PCS plus left lobe hepatectomy (n = 3, red line).

care takers. The surgical area (abdomen) was initially shaved and extensively scrubbed with povidone. The animals were prepped and draped in a sterile fashion after being stable under general anesthesia. The abdominal cavity was entered through a midline incision. Abdominal retractors were used for further surgical exposure. The liver hilum was exposed, and the left lateral segment (LLS) vasculature was isolated. The LLS was excised in a bloodless manner through the use of a reticulated stapler (Ethicon Inc., Somerville, NJ). The LLS was perfused ex vivo through the left PV with ringer lactate at 4°C and subsequently packed in an ice container for subsequent cell isolation. The right PV was properly isolated and further ligated (RPVL) prior to hepatocyte autologous infusion. The PCS was performed after complete isolation of the main PV beyond the confluence between the splenic and superior mesenteric veins (SMVs). The infrahepatic inferior vena cava (IVC) was isolated and encircled by vascular tape. The main PV was transected at the bifurcation level with a reticulated stapler (Ethicon) after previous proximal clamping at the SMV/splenic vein confluence. A vascular clamp (Satinsky, Medline Industries Inc, Northfield, IL) was placed to allow partial clamping of the IVC. An end-to-side anastomosis (6-0 Prolene running suture) was performed between the main PV and the IVC after proper positioning and intraluminal flushing with heparinized saline solution. The clamps were removed after the completion of the PCS, and additional hemostasis was performed. A central intravenous (IV) access (Broviac, BD, Covington, GA) was placed into the superior vena cava for the postoperative care.

HEPATOCYTE ISOLATION AND TRANSPLANTATION

The cold ischemia time for the left liver lobe was <2 hours after the left lateral lobe hepatectomy (LLH). The liver segment was flushed with cold lactated Ringer's solution in the back table, packed in a double sterile plastic bag with ice, and sent to the laboratory at 4°C for subsequent hepatocyte isolation. Hepatocytes were isolated using a method derived from the 2-step collagenase perfusion procedure[24] with a viability over 90% and with a cellular mix containing more than 90% hepatocytes. The animals remained in the operative room (OR) under general anesthesia during the cell isolation procedure (approximately 4 hours). The hepatocytes were transported back to the OR from the cell transplant facility in a cooler at 4°C. Separate 5-mL syringes were used for cell infusion under sterile technique. Isolated hepatocytes (0.3 to 1.8 × 10^9 cells) were transplanted into 3-18 periportal/mesenteric LNs using 23- to 25-gauge needle syringes (25 to 50 × 10^6 cells/mL) under direct vision. Capsular hemostasis was briefly performed with electrocautery (Bovie Medical Corporation, Melville, NY). No immediate intraoperative complications from the repeated hepatocyte intraparenchymal LN infusions were observed. The abdominal cavity was profusely irrigated with antibiotics and antifungal solutions after meticulous hemostasis had been achieved. The abdominal wall was closed in a 2-layer fashion. A sealing surgical dressing was placed (3M, Saint Paul, MN) over the skin closure. Experimental animals were properly killed at 30 days (n = 4) and 60 days (n = 2) after transplantation for the end-study necropsy (Table in Fig. 1B).

TABLE 1. Definition of Genes Investigated

Gene Symbol	Gene Name	Assay ID
ALB	Albumin	Ss03378640_u1
CYP1A2	Cytochrome P450, family 1, subfamily A, polypeptide 2	Ss04246175_m1
ASGR1	Asialoglycoprotein receptor 1	Ss04327457_m1
OTC	Ornithine carbamoyltransferase	Ss03374894_m1
CYP7A1	Cytochrome P450, family 7, subfamily A, polypeptide 1	Ss03378689_u1
CYP27A1	Cytochrome P450, family 27, subfamily A, polypeptide 1	Ss03377319_u1
ABCB1	ATP binding cassette subfamily B member 1	Ss03373436_m1
ABCC2	ATP binding cassette subfamily C member 2	Ss03373436_m1
DPP4	Dipeptidyl peptidase-4	Ss03383683_u1
LYVE1	Lymphatic vessel endothelial hyaluronan receptor 1	Ss03376355_u1
EpCAM	Epithelial cell adhesion molecule	Ss03384752_u1
PPIA	Peptidylprolyl isomerase A	Ss03394782_g1
ACTB	Actin Beta	Ss03378640_u1

POSTOPERATIVE CARE

The animals were allowed to recover from anesthesia with appropriate monitoring and resume spontaneous ventilation. They received daily IV antibiotics and additional medication by mouth twice a day. Postoperative care of the animals was under the direction of the medical team and staff veterinarians. All animals received postoperative Banamine (Merck Animal Health, Madison, NJ; flunixin meglumine, 2.2 mg IV, intramuscular once every 6 hours) for analgesia. Animals

were monitored 24 hours/day by trained intensive care unit staff (Critical Care Technicians) from McGowan Institute for Regenerative Medicine (Pittsburgh, PA). Liver function tests were obtained daily for the first 10 days and up to 30 or 60 days. Animals experiencing signs of hepatic encephalopathy (HE) and high serum ammonia levels were successfully treated with lactulose (30 mL per os [po] 3 times a day) or neomycin (500 mg po quater in die) if showing signs of intractable diarrhea. Early laboratorial evidence of massive hepatocellular necrosis (significantly high aspartate aminotransferase [AST] and alanine aminotransferase [ALT] serum levels) led to transient hepatic insufficiency but not to liver failure.

END STUDY PROCEDURES AND EXPLANT PROTOCOL

Each animal underwent a complete necropsy examination at the end of its established protocol. At 30-60 days after transplant, glucose was administered according to the results of the blood sample analysis and the general state of the animal, taking into particular consideration whether it was eating and drinking freely. Thiopental (lethal dosage) was given intravenously using the established central vein cannula to initiate euthanasia. Subsequently the animals had potassium chloride administered at a lethal dose to achieve cardiac arrest and electrocardiogram silence. A complete necropsy was conducted focusing on the transplanted LNs. The native liver was removed, examined, weighed, and processed for histology. Any gross change was described and photographed.

BIOCHEMICAL ANALYSES OF BLOOD SAMPLES

Blood collection was performed every day for the first 10 days and at 30 days after surgery. Porcine ALT, AST, alkaline phosphatase (ALP), total bilirubin, direct bilirubin, gamma-glutamyl transpeptidase (GGT), and ammonia concentration were measured by enzyme-linked immunosorbent assay (ELISA).

HISTOLOGICAL ANALYSES AND IMMUNOSTAININGS

Tissues were fixed in 4% paraformaldehyde (PFA) for 4 hours, infiltrated in 30% sucrose for 12 hours, and then embedded in optimal cutting temperature medium, frozen, and stored at −80°C. Alternatively, following 24 hours of PFA incubation, tissues were embedded in paraffin. Histological stains (hematoxylin-eosin [H & E], Oil Red O, and Masson's trichrome staining) were performed in paraffin-embedded sections, as described elsewhere. For fluorescent immunohistochemistry staining, frozen sections were rehydrated with phosphate-buffered saline (PBS) and blocked with 5% bovine serum albumin (BSA) or milk for 30 minutes. Sections were then incubated with primary antibody for 1 hour followed by incubation with Alexa Fluor 488 and/or 594 conjugated secondary antibody (Invitrogen Corporation, Carlsbad, CA) for 30 minutes. Sections were mounted with Hoechst (Hoechst 33342, Trihydrochloride, Trihydrate, Thermo Fisher Scientific, Waltham, MA)-containing mounting media. For chromogenic immunohistochemistry staining, paraffin sections were deparaffinized in xylene and rehydrated in graded alcohol. Endogenous peroxidases were blocked using 3% hydrogen peroxide for 10 minutes. Antigen unmasking was performed using 10-mM sodium citrate buffer with pH 6.0. Nonspecific binding was blocked by incubating the slides in 3% BSA in PBS supplemented with 0.05% Tween 20 (Thermo Fisher Scientific) for 30 minutes. The slides were exposed to primary antibodies overnight at 4°C, incubated with biotinylated secondary antibody and later incubated with streptavidin horseradish peroxidase; 3,3´-diaminobenzidine was used as a chromogen. Immunostained sections were counterstained with Mayer's (Sigma-Aldrich Chemicals Company, St. Louis, MO) hematoxylin and mounted in Permount mounting medium (Thermo Fisher Scientific). Images were captured with an Olympus IX71 (Olympus Corporation, Shinjuku City, Tokyo, Japan) inverted microscope.

ANTIBODIES

The following reagents were purchased for immunohistochemistry in porcine tissues: ER-TR7, α smooth muscle actin (α-SMA), CD31, E-cadherin, Ki-67 (Abcam, Cambridge, UK); cytokeratin (CK) 18 (Chemicon International, Thermo Fisher Scientific); peripheral node addressin (PNAd), (BD Biosciences, Franklin Lakes, NJ); albumin (ALB; Bethyl Laboratories, Montgomery, TX); and cytochrome P450 7A1 (CYP7A1), cytochrome P450 27A1 (CYP27A1), multidrug resistance–associated protein 2 (MRP2), bile salt export pump (BSEP), CK7, and CK19 (Santa Cruz Biotechnology, Dallas, TX).

MESSENGER RNA EXPRESSION OF LIVER-RELATED GENES

Total RNA was isolated from the normal liver and LNs of a nontransplanted swine and from an ectopic and native liver of P147-13 using the RNAeasy kit (Qiagen, Hilden, Germany). RNA was quantified with the Nanodrop 2000c Spectrophotometer (Thermo Scientific). Reverse transcription was performed using TaqMan Universal polymerase chain reaction (PCR) Master Mix (Life Technologies, Carlsbad, CA) followed by real-time PCR on an StepOne Plus real-time PCR thermal cycler (Applied Biosystems, Foster City, CA). TaqMan probes and primers were purchased from Life Technologies (Table 1). Expression was normalized to β-actin (ACTB). Values represent mean ± standard deviation (SD; n = 3 in each group).

TISSUE BILE ACID MEASUREMENT

Tissues were rinsed in ice-cold PBS, minced to small pieces, and then homogenized in 500 μL PBS by ultrasonication. The homogenates were centrifuged for 15 minutes at 5000 rpm. Total bile acid (TBA) was measured in the supernatant by ELISA (BlueGreen Biotech, Shanghai, China), following the manufacturer's protocol.

Results

ANIMALS

All animals survived the operative procedures and had no surgical complications. They displayed a transient weight loss with reversible mild-to-moderate hepatocellular damage, while showing signs of HE and laboratorial evidence of massive hepatocellular necrosis. The RPVL animals with LLH (n = 3) were killed 30 days after LN injections. RPVL animals were clinically stable while showing signs of moderate HE, which was well controlled with continuous administration of lactulose and neomycin. The PCS animals with LLH were sacrificed 30 days (n = 1) and 60 days (n = 2) after LN injections, respectively (Table in Fig. 1B). These 3 animals showed moderate HE and hepatocellular damage by laboratorial parameters. Eventually, all 6 animals included in this study showed clinical and laboratory signs of progressive recovery from the surgically induced hepatocellular insult.

BIOCHEMICAL ANALYSES OF BLOOD SAMPLES COLLECTED DURING THE EXPERIMENTS

Liver function tests showed a classic pattern of hepatocellular necrosis in both groups. Transient elevations of ALT, AST, and ALP were a direct consequence of the liver injuries induced by the lack of portal flow, with the PCS group showing slightly more severe liver injuries than RPVL group (Fig. 1C). As expected, elevations in serum total and indirect bilirubin were higher after the PCS. Direct bilirubin and GGT were similar in both groups. Surprisingly, the PCS animals rapidly restored most of their liver functions similarly to the RPVL animals, indicating the possible regeneration of hepatocellular mass lost in both groups.

HEPATOCYTE ENGRAFTMENT IN LNs AFTER RPVL AND LLH

CK18 was used as a hepatocyte marker during the initial immunohistological analysis. The positive control staining was established with the native liver, and the negative control staining was established with the normal LNs (Fig. 2A). ER-TR7, a marker of reticular fibroblast, was used to contrast CK18+ hepatocytes with the connective tissues delineating swine hepatic lobulation patterns. Additionally, α-SMA and CD31 were used to assess the vasculatures in the different tissues collected, and PNAd was staining for high endothelial venules in LNs (Fig. 2A).

The transplanted LNs were identified by surgical clips placed after the initial cell injections (Fig. 2B). Macroscopic signs for the presence of ectopic hepatic tissue were consistently observed and initially seen as small red/brown patches within the parenchyma of the transplanted LNs. These ectopic sites of hepatic tissue were further identified by histology as clusters of CK18+ and E-cadherin+ hepatocytes mostly under the LN capsule (Fig. 2C). The engrafted ectopic hepatocytes were close to α-SMA+ vessels, but lacking a complete morphology of swine hepatic lobules. ER-TR7 staining was dispersed around CK18+ hepatocytes, revealing additional signs of immature liver tissue. Furthermore, the proliferation marker Ki-67 was absent in hepatocytes engrafted into the LNs but was positive in lymphoid germinal centers, indicating that the RPVL created a transient ischemic event to the liver parenchyma, which was short lived. This result indicates the lack of further stimulation

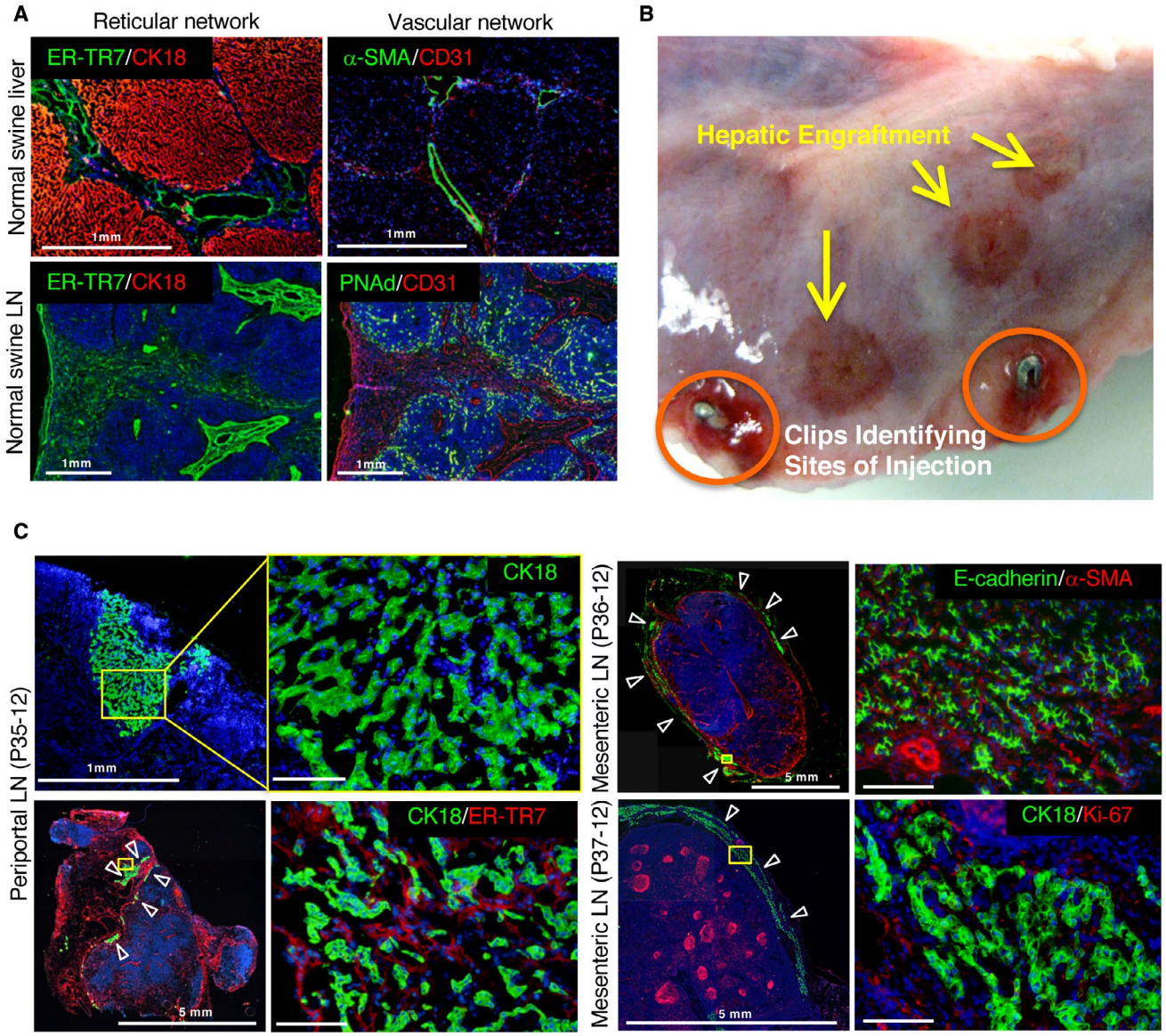

FIG. 2. Liver tissue generated by hepatocyte transplantation in LNs of pigs undergoing RPVL and partial hepatectomy. (A) Reticular and vascular networks in control pig liver and LN. Normal pig native liver immunostained for hepatocytes with (top left) CK18 (red) and for reticular fibroblasts and fibers (ER-TR7, green) and (top right) endothelial cells (CD31, red) or hepatic artery/PV with α-SMA (green). Normal pig LN stained with (bottom left) CK18 (red) and ER-TR7 (green) or (bottom right) CD31 (red) and high endothelial venules (PNAd, green). (B) Macroscopic view of a transplanted LN with surgical clips (circled in orange) to identify the sites where the hepatocytes were injected. Additional hepatic engraftments are observed on the surface of the LN and are indicated by yellow arrows. (C) Immunostaining of the engrafted hepatocytes in LN from transplanted animals P35-12, P36-12, and P37-12. The yellow rectangles highlight the area of magnification presented on the right side of the panel. (left) P35-12: general view of the injected LN and the limited engraftment of hepatocytes (CK18, green). White arrowheads indicate hepatocyte engraftment in a LN. (right) General view and higher magnification of the injected LN for P36-12 (top) and P37-12 (bottom). E-cadherin and CK18 (green) stained the hepatocytes; α-SMA (red) stained the vasculature; and Ki-67 (red) stained the proliferating cells. All immunostainings were counterstained with Hoechst 33342 dye. Scale bar, 100 μm or as indicated.

for ectopic hepatocyte proliferation beyond 30 days in the RPVL animals. Our initial findings in the RPVL group suggested that transplanted hepatocytes can engraft, survive up to 30 days, and form some poorly organized hepatic tissue in the LNs. However, the size of the hepatic engraftment appears to be limited by the

magnitude of the hepatic injuries induced in this swine model.

HEPATOCYTE ENGRAFTMENT IN LNs AFTER PCS AND PARTIAL HEPATECTOMY

The PCS group was expected to be more effective than the RPVL for hepatocyte engraftment because it caused extended and sustained hepatocellular injury due to the complete lack of portal flow. At 1 month after liver cell transplantation, macroscopic signs of hepatocyte engraftment characterized by dark red tissue were clearly observed within the parenchyma of the injected LNs (Fig. 3A, left image, yellow arrows). CK18+ and E-cadherin+ hepatocytes were identified at these locations forming hepatic tissues, with a sagittal thickness up to 500 μm (Fig. 3A, middle images). The presence of Ki-67+ proliferating hepatocytes at the site of engraftment after 30 days was an indication that induced hepatic injury was still present in the PCS animals when compared with RPVL animals (Fig. 3A, right image). Because of these encouraging data with the presence of actively dividing hepatocytes, the last 2 animals were killed 2 months after hepatocyte injection. At necropsy, the injected LNs were identified and sliced longitudinally to macroscopically observe the presence of ectopic hepatic tissue (Fig. 3B, left image). A much larger mass of hepatic tissue, over 1 mm in thickness, was identified in LNs by its red color. Moreover, immunostaining analyses of frozen sections using CK18/ER-TR7 detected the presence of normal hepatocytes properly organized within a normal swine cytoarchitecture in the formation of hepatic lobules (Fig. 3B, middle image), while displaying normal swine sinusoidal and presumptive central vein histological features. However, Ki-67 was not expressed in these hepatocytes, indicating a lack of further hepatic proliferation at 60 days in the PCS group (data not shown).

In the last animal with PCS (P147-13), devascularization of the right and middle hepatic lobes conducted during the initial procedure generated additional liver injuries and prevented potentially the formation of perihepatic portal venous shunts toward the liver capsule. In this animal, the regenerative response of the transplanted hepatocytes was even more robust, with large patches of hepatic tissues being identified 60 days after the initial transplant. Interestingly, an increased thickness on the LN-bounded ectopic hepatic tissue up to several millimeters was clearly detectable with feeder vessels (Fig. 3C, left images; Fig. 4B, for tissue thickness summary) when compared with previous specimens. A representation of 4 transplanted LNs collected and immunostained with CK18/ER-TR7 showed a 43%-67% presence of hepatocytes per tissue section, with a weight of 2.3-5.7 g for the entire LN mass (Fig. 4C, lower left images). An estimated 30 g of ectopic liver tissue mass was regenerated in this animal, which represented approximately 2% of the 1.5-kg native liver collected at the time of necropsy. Furthermore, similar to the control normal swine liver tissue, the presence of distinct hepatic lobules was observed by histology in the newly developed ectopic livers within the transplanted mesenteric LNs (Fig. 3C, right top and bottom images). In addition, organized neovascularization containing red blood cells was identified at high magnification in these perisinusoidal spaces, which were very similar to what was observed in the control liver (Fig. 3D). Interestingly, the development of hepatocellular steatosis, a common feature observed in hepatic segments after portosystemic shunt, was present in the native liver but was not found in the ectopic liver tissues generated in the mesenteric LNs (Fig. 3D).

The presence of hepatic lobular configurations in the ectopic livers at 60 days after hepatocyte transplantation was confirmed by Masson's trichrome stain (Fig. 4A), outlining the normal hepatic–like collagen features in the new extracellular matrix developed after the initial ectopic hepatocyte engraftment into the LNs. Masson is a standard staining for the liver extracellular matrix, revealing specific features of hepatic scaffold anatomy, where the presence of collagen fibers from the newly formed hepatic lobules is shown by the red background of hepatocytes surrounded by blue-colored collagen, along the perisinusoidal spaces. These classic structural features of hepatic lobular anatomy were clearly demonstrated to be present in the ectopic liver developed within the LN after hepatocyte transplantation. However, the staining with glutamate synthetase, which was positive in the ectopic liver of the tyrosinemic mouse,[22] is not positive in our pig's model (not shown), indicating a potential immaturity in the lobule formed. We hypothesized that the timing of the termination of the experiment (2 months) and the regeneration of the native liver may have prevented full maturation of the ectopic liver.

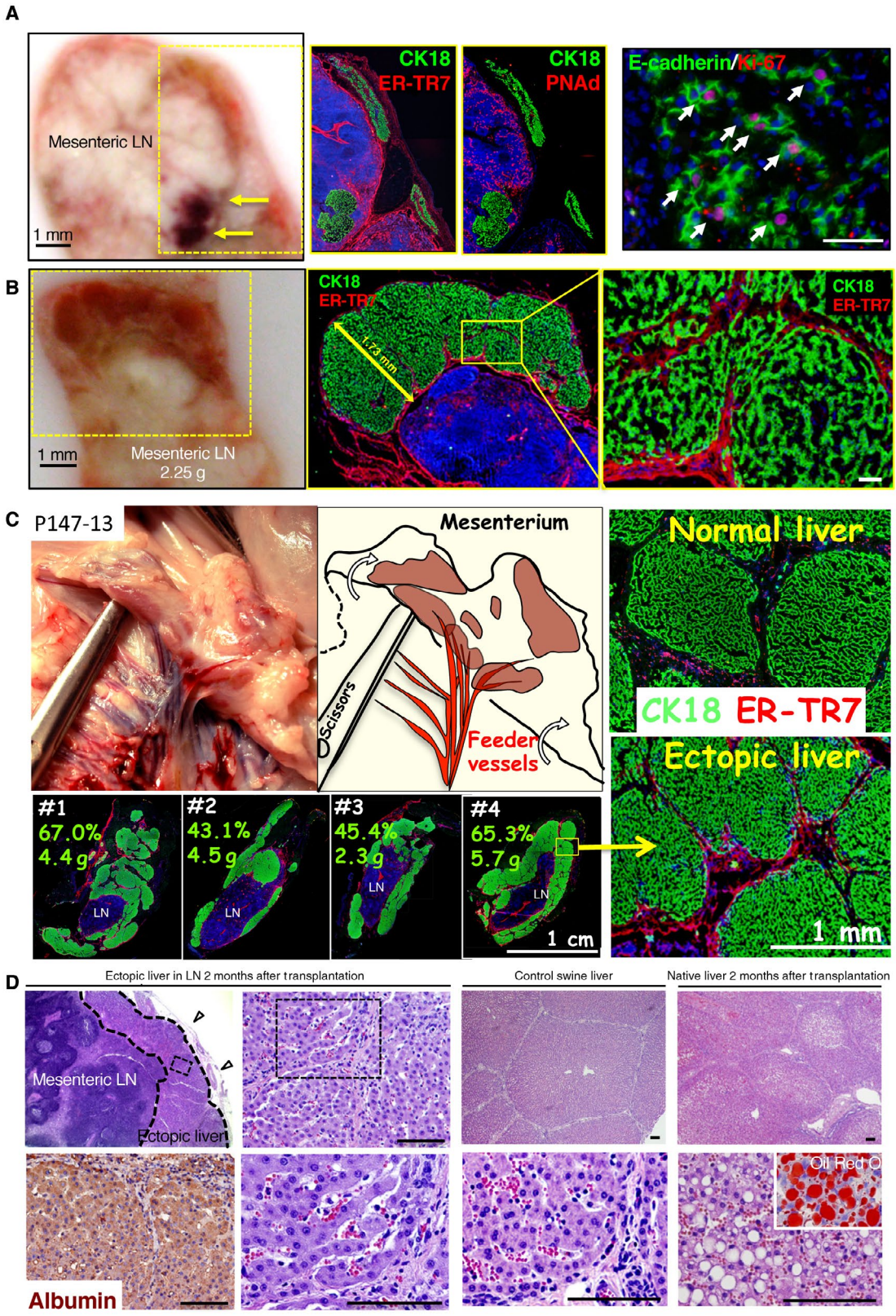
A
Mesenteric LN
1 mm
CK18
ER-TR7
CK18
PNAd
E-cadherin/Ki-67
B
1 mm
Mesenteric LN
2.25 g
CK18
ER-TR7
1.73 mm
CK18
ER-TR7
C
P147-13
Mesenterium
Scissors
Feeder
vessels
Normal liver
CK18 ER-TR7
Ectopic liver
1 mm
#1
67.0%
4.4 g
LN
#2
43.1%
4.5 g
LN
#3
45.4%
2.3 g
LN
#4
65.3%
5.7 g
LN
1 cm
D
Ectopic liver in LN 2 months after transplantation
Control swine liver
Native liver 2 months after transplantation
Mesenteric LN
Ectopic liver
Albumin
Oil Red O

FIG. 3. Hepatocyte engraftment in LNs after PCS and partial hepatectomy. (A) Macroscopic view of the sagittal section of the liver of pig P148-12 LN at 30 days after hepatocyte transplantation. The yellow arrows indicate the presence of highly vascularized hepatic engraftment. The yellow rectangles indicate the area of magnification presented in the panels to the right. The immunostaining of the frozen sections with CK18 and E-cadherin (green) highlights the presence of hepatocytes; ER-TR7 (red) indicates the reticular fibroblasts and fibers; PNAd (red) shows the high endothelial venules; and Ki-67 (red) shows the proliferating cells. (B) Macroscopic view of pig P194-12 LN 60 days after hepatocyte transplantation. Frozen sections were stained with CK18 (hepatocytes, green) and ER-TR7 (reticular fibroblasts and fibers, red) and underscore the presence of hepatic lobules. (C) Macroscopic view of the abdominal region of pig P147-13 at 60 days after hepatocyte transplantation and in the place where hepatic engraftment was localized. A graphic drawing pointed out the presence of ectopic hepatic tissue with large vasculature. Frozen sections of normal native liver and ectopic liver tissue in LN were stained with CK18 (green) and ER-TR7 (red) to demonstrate the similar architecture of the pig hepatic lobules in normal native liver and in ectopic liver tissue. Four different LNs from the same animal were immunostained with CK18/ER-TR7 to show a similar engraftment in different LNs. The numbers represent the percentage of estimated engraftment of hepatic tissues per LN as well as the weights of isolated LNs. (D) (first and second columns) Paraffin-embedded sections of P147-13 LN with H & E showing the localization of ectopic tissue under the LN capsule (open arrowheads) as well as higher magnification of the rectangle with dotted lines demonstrating microvascularization between the hepatic plates with the presence of red blood cells. An ALB staining of the ectopic liver tissue is also shown. (third column) The control native liver H & E at low and high magnification. (fourth column) H & E of the native liver of pig P147-13 at low and high magnification showing vacuolated hepatocytes. The inserted picture after Oil Red O staining demonstrates the presence of fat and lipids in vacuolated hepatocytes of the native liver following PCS. Counterstaining for panels A-C was done with Hoechst 33342 dye. Scale bar, 100 μm or as indicated.

Important information regarding the volume of the ectopic livers was further assessed indirectly through the measurement of the thickness of ectopic liver tissues engrafted into LNs (Fig. 4B). In the RPVL animals, the thickness of ectopic liver tissue was limited to approximately 500 μm and was similar across all 3 animals in this group. In contrast with the PCS animals, ectopic liver tissue thickness was increased from >500 μm at 30 days to several millimeters at 60 days, particularly after the additional liver injury performed in the third animal (P147-13). These results indicate that the level of native liver injury was apparently driving the regenerative potential of ectopic liver growth. However, a surprising outcome was the absence of Ki-67+ hepatocytes 60 days after PCS. This observation suggested a loss of stimuli for hepatocyte proliferation and liver tissue growth in the PCS group once the lack of portal flow was fully compensated by intrahepatic shunts developed within the right lobe along the IVC. To quantify the regeneration of the native livers after the devascularization procedures, these specimens were weighed and further examined after the end-study necropsy. Both morphology and weight revealed a compensatory growth of the remaining native liver, regaining an average 1.5 kg expected liver mass for pigs weighing approximately 70 kg on average (Fig. 4C). This finding was not particularly surprising in the swine model, despite the complete lack of portal flow through the native PV after the PCS. The IVC is completely engulfed by the right hepatic lobe, which allows a close to full restoration of trophic portal flow to the right lobe through the formation of new intrahepatic shunts after a complete PCS. The liver-wrapped IVC would explain the compensatory growth observed after PCS, limiting longterm studies with this swine model.

ECTOPIC LIVER FUNCTION IN THE PIGS AFTER THE PCS

The ectopic livers presented similar histological morphology to the native healthy livers, regarding ALB expression and glycogen storage (Fig. 3D and not shown). More importantly, bile duct cells and the neoformation of biliary ducts were clearly identified in and around the ectopic liver tissues developed in the LNs (Fig. 5A,B). This observation is different from our previous experience because no bile duct cells were identified in our mouse models of ectopic livers.[22,23] Both intrahepatic and extrahepatic CK19+ and CK7+ bile duct cells were detected in the swine ectopic livers (Fig. 5A,B).

Next, to determine if bile acids were being accumulated into the LN-bounded ectopic livers, bile acids were quantified in and around ectopic liver tissue. This analysis included the native liver, the ectopic liver, the engrafted LN (after removal of the ectopic liver tissue), and nonengrafted LN from experimental animal P147-13. A control (native) liver tissue was collected and used from a control pig. Analyses for the presence of bile acids revealed no accumulation in the ectopic livers, suggesting bile secretion and extrahepatic transportation outside the ectopic liver tissue (Fig. 5C). In addition, no signs of intrahepatic cholestasis were observed in the ectopic liver

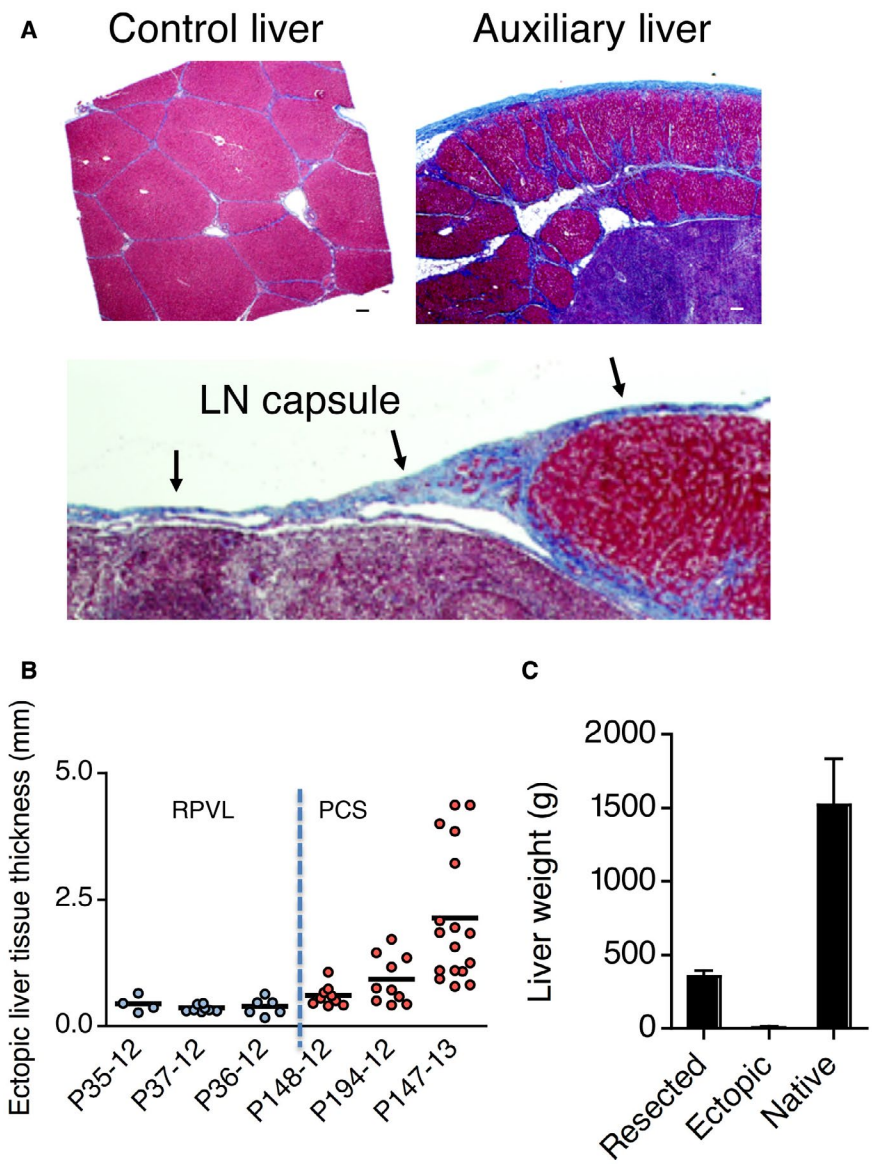

FIG. 4. Development of an auxiliary liver in pig LNs. (A) Masson's trichrome stain to show the presence of liver lobules surrounded by blue colored collagen in (top left panel) the control liver and (top right and lower panel) auxiliary liver in LN. (B) Summary of hepatocyte engraftment in LNs by ectopic liver tissue thickness. (C) Weights of resected liver lobe, ectopic liver tissues, and native livers collected after each necropsy. All 6 experimental animals were used for this graph and presented as mean ± SD. Scale bar, 100 μm or as indicated.

tissue (Fig. 5A). To assess further molecular functions of the ectopic livers, messenger RNA (mRNA) expression of liver-related genes was quantified. The mRNA levels of ALB, asialoglycoprotein receptor 1 (ASGR1), ornithine carbamoyltransferase (OTC), CYP1A2, and dipeptidyl peptidase-4 (DPP4) in the ectopic livers were lower but were present when compared with those in the control native liver (Fig. 5D). These results could be explained to some extent by a potential dilution of the remaining lymphoid tissues still present in the hepatized LN tissue analyzed, as well as the use of β-actin expression for normalization. The expression levels of genes associated with the synthesis of bile acids from cholesterol and their secretion were also examined (Fig. 5D). Specifically, we focused on 2 members of the cytochrome P450 gene family: CYP7A1, codifying for a rate-limiting enzyme in the synthesis of bile acid from cholesterol

and CYP27A1, codifying for an enzyme prominently involved in the biosynthesis of bile acids.

Also, we examined 2 genes with products that are important for bile acid transports: ATP binding cassette B1 (ABCB1) and ATP binding cassette C2 (ABCC2). We found these genes to be all expressed in the ectopic livers. In addition, immunostaining of BSEP as well as CYP7A1, CYP27A1, and ABCC2

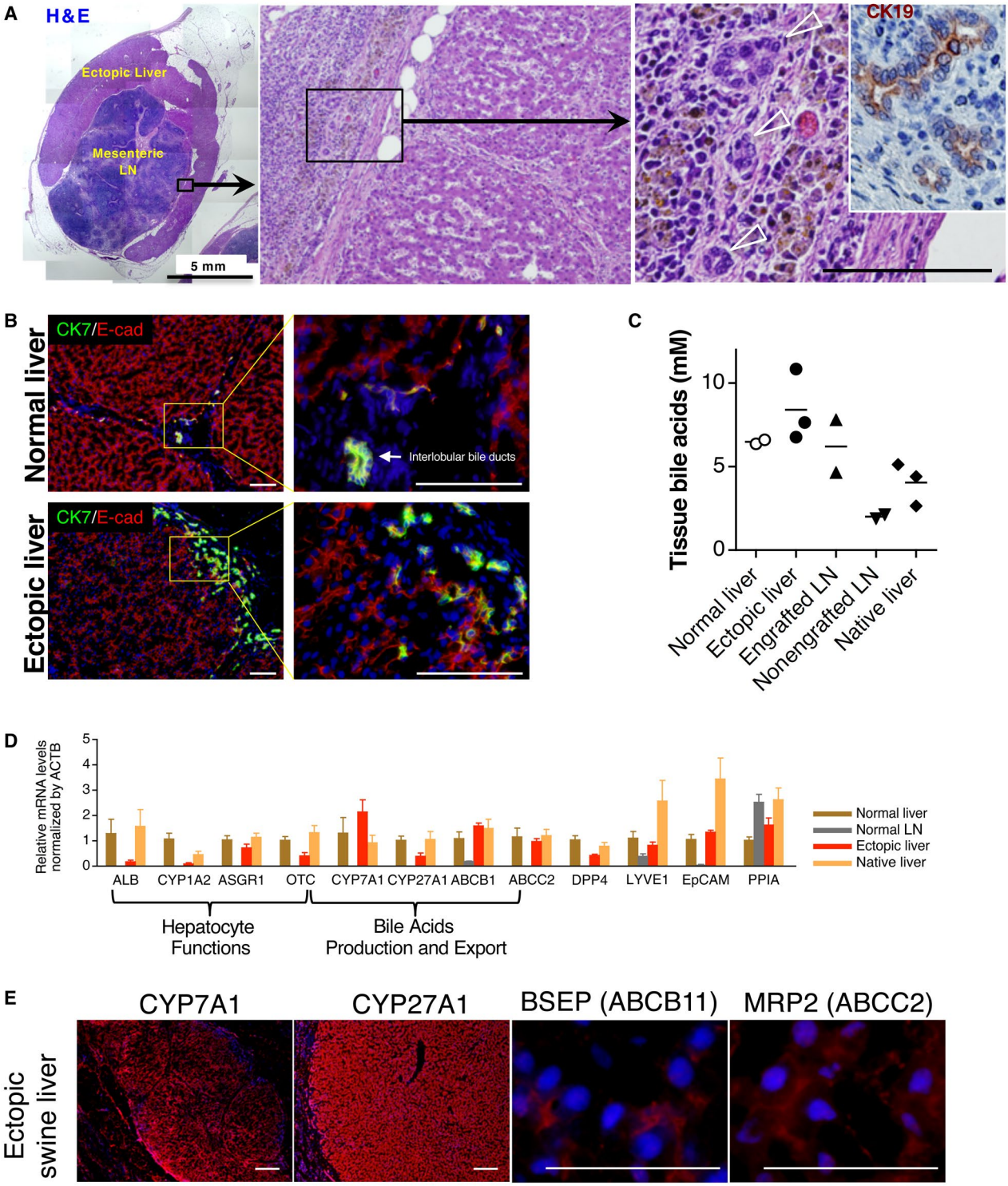

FIG. 5. Auxiliary liver and biliary system. (A) Whole liver tissues engrafted in a LN of animal P147-13. Multiple pictures of H & E staining were taken to present the whole engrafted liver tissue in LN. The black rectangle indicates the area of magnification presented in the middle panel and the location where small bile ducts were identified, outside of the hepatic engraftment. In the left panel, the inset is a CK19 staining (brown) on a serial paraffin-embedded section identifying bile ducts. (B) Immunostaining of frozen sections from ectopic and control liver showing the presence of CK7+ bile duct cells, as well as the presence of intrahepatic ducts. (C) Tissues bile acid analyses. Bile acids were quantified in the normal (native) liver, ectopic liver, engrafted LN (without ectopic liver tissue collected), nonengrafted LN (in the experimental animals), and native liver (in the experimental animals). (D) The mRNA expression by quantitative polymerase chain reaction of ALB, CYP1A2, ASGR1, OCT, CYP7A1, CYP27A1, ABCB1, ABCC2, DPP4, LYVE1, EpCAM, ACTB, and PPIA; n = 3 per group, presented as mean ± SD. (E) Immunostaining of CYP7A1, CYP27A1, BSEP, and MRP2 (ABCC2) on frozen sections of the ectopic liver (red). All immunostainings were counterstained with Hoechst 33342 dye. Scale bar, 100 μm or as indicated.

showed positive hepatocyte (Fig. 5E), reinforcing our findings regarding the integrity of some biliary secretion pathways in the ectopic livers. These results were consistent with the bile acid levels present in the ectopic liver, which were at similar levels to the normal liver (Fig. 5C). This outcome suggests that hepatocytes in the ectopic livers were able to metabolize cholesterol into bile acids then to export these bile acids, possibly through newly formed CK7+/CK19+ bile ducts.

Discussion

Livers and LNs are unique organs with complementary cell biology features, as the former can regenerate effectively while the latter can nurture cell growth and expansion continuously as a natural bioreactor. By transplanting hepatocytes into LNs, we had previously demonstrated our ability to regenerate anatomically and histologically functional ectopic liver tissues, which act as auxiliary livers capable of rescuing tyrosinemic mice from a lethal liver disease.[22,23] In the present study, our goal was to demonstrate that hepatocytes transplanted in large animal models of liver disease, different from tyrosinemia, could also engraft within the LN and could organize into complex ectopic liver tissues with normal cytoarchitecture such as liver lobules and microvascularization. Our swine models of subacute liver failure are more clinically relevant to patients experiencing progressive liver failure than tyrosinemic models because reliable large animal models for ESLD remain elusive. In addition, swine and human livers have several anatomical similarities that create unique opportunities for proof-of-concept preclinical experiments regarding innovative hepatobiliary therapies.

PCSs have been extensively used as a reliable model for subacute liver failure in large animals. Furthermore, portosystemic shunts have evolved clinically into more selective and minimally invasive procedures, such as the transjugular intrahepatic portosystemic shunt, which became the standard of care in a selected group of patients with ESLD that was complicated by portal hypertension. We also used our knowledge in auxiliary liver experimentation, where important concepts of hepatotrophic factors and feedback regulation between native and ectopic liver segments have been elegantly documented in the past.[25,26] These PCS experiments were an attempt to create the proper conditions for ectopic hepatocyte regeneration and growth in a challenging environment for the native liver experiencing the acute interruption of effective portal flow followed by massive hepatocellular necrosis and potential subhepatic failure. However, this model, which simulates early hepatocyte engraftment and proliferation after transplantation, also lacks a prolonged up-regulation of hepatic regeneration.

During the course of moderate hepatic damage, we showed that autologous hepatocytes transplanted into LNs have the ability to proliferate and, subsequently, to organize into functional vascularized ectopic liver tissues containing hepatic lobulation and neoformed biliary structures. Our results demonstrated the validity in our approach of transplanting hepatocyte into the LNs with the newly developed hepatic tissue responding positively to hepatic injury as previously seen in auxiliary liver models. The well-described hepatostat feedback regulation mechanism involving the native liver is capable of both promoting and limiting ectopic liver growth,[27] as subsequent native hepatic regeneration and compensatory growth can limit the growth of the ectopic liver downstream by direct hepatocellular competition.

In this swine model, the histological evidence of biliary duct structures associated with the basic biliary functions confirmed by transcriptional and metabolic assays reinforces our conviction about the feasibility of organogenesis driven by cell transplantation into the LNs as natural bioreactors. The presence of biliary cells may have come as a contaminant from the isolated liver cells infused into the LNs. However, recent evidence has suggested the origin of induced biliary differentiation from early progenitor cells[28] while others have proposed transdifferentiation from hepatocytes.[29]

Interestingly, ectopic liver tissues have a similar to slightly higher level of TBA when compared with a normal liver, suggesting that bile acids are produced by hepatocytes in the ectopic liver and transported out of the newly formed hepatic lobules, possibly through neoformed biliary ducts. The apparently physiological bile efflux from the ectopic liver tissue could be draining into the intestinal lumen through newly formed septal/area/segmental ducts seen macroscopically during the necropsy as potential microenteric lymphatic-biliary fistulas. Although we detected the presence of cholangiocytes and bile duct structures in the PCS swine model, confirmed the presence of bile acid transporters, and detected no accumulation of bile acids in the ectopic liver, we have no data to indicate their functionality in bile flow, from secretion to excretion. The LNs containing ectopic hepatic tissue did not show any macroscopic signs of bilomas during the necropsy. Rather, these LNs showed very fine white strings of lymphatic tissue, resembling the internal microbiliary-enteric fistulas seen in patients with biliary atresia years after a Kasai procedure has been performed.[30] Interestingly, the lymphatic transport of bile acids has been reported previously in humans,[31-34] suggesting that direct uptake of bile acids in the intestinal lymph is also possible.

Our study describes, for the first time, engraftment of hepatocytes into LN of a large animal with the development of ectopic liver tissue that is independent from tyrosinemia. This result complements our previously published work with the tyrosinemic mouse model.[22,23] Our experimental pigs as models of acute liver damage were not designed to simulate massive liver loss but rather the induction of acute hepatocellular necrosis as a driving force for active but limited liver regeneration. Our preclinical experiments were aimed to show the safety and the feasibility of engrafting hepatocytes in the LNs of animals experiencing acute hepatocellular necrosis through the derivation of the main PV flow into the vena cava. The LNs where the hepatocytes engrafted showed increased size and possible blood flow from the local circulation, as a compensatory mechanism for the acute decrease of functional hepatocellular mass. However, the regenerative process in our pig models was of a short duration, which explains the relatively small size of the ectopic liver tissue in LN when compared with the tyrosinemic mouse. For example, P147-13, the animal with the largest ectopic liver mass in LNs, had approximately 30 g or 2% of the native liver mass, possibly limited by the compensatory growth of the native liver that had regained its normal weight. This limited the growth of the ectopic liver mass in our pig model, which resulted in an inability to demonstrate the functionality of the transplanted hepatocytes as well as a difficulty in demonstrating the level of ectopic liver support that would be expected for patients with ESLD. Interestingly, in some patients with liver diseases, proliferation of hepatocytes in their native diseased liver has been reported previously,[35-37] and on the basis of our previous observations in animal models, we envision that transplantation of hepatocytes into the LNs of patients suffering from advanced liver disease could result in a more robust engraftment, proliferation, and expansion of hepatocytes to form functional auxiliary liver tissue.

For subsequent clinical applications of this combined approach of organogenesis and auxiliary liver development through hepatocyte transplantation into the LNs, additional preclinical studies will be necessary to determine if allogeneic hepatocytes can properly engraft and grow when facing major histocompatibility issues requiring the use of nonspecific immunosuppressive therapy. We previously showed that allogeneic mouse hepatocytes could engraft and develop in an allogeneic ectopic liver in a mouse LN,[23] but many factors can influence the survival of the transplanted allogeneic human hepatocytes, which will require a very focused initial target population in humans experiencing liver diseases. We are currently completing additional large animal studies using standard immunosuppression therapy in a fully mismatched allogeneic combination, where new options for cell injection are also being tested.

Moreover, a recent clinical trial of transplanting a very large number of allogeneic hepatocytes into the portal flow resulted in a robust acute cellular rejection and graft failure, potentially raising the question about the ideal route for hepatocyte transplantation away from the hepatic sinusoidal endothelial system.[38] Direct intraparenchymal hepatocyte transplantation into the LNs might allow better initial cell engraftment and the subsequent induction of peripheral tolerance, becoming a less immunogenic transplantation approach site when compared with direct hepatocyte injection within the portal circulation.[39]

REFERENCES

1) Tapper EB, Parikh ND. Mortality due to cirrhosis and liver cancer in the United States, 1999-2016: observational study. BMJ 2018;362:k2817.

2) Starzl TE, Groth CG, Brettschneider L, Penn I, Fulginiti VA, Moon JB, et al. Orthotopic homotransplantation of the human liver. Ann Surg 1968;168:392-415.
3) Reuben A. Alcohol and the liver. Curr Opin Gastroenterol 2007;23:283-291.
4) Perkins JD, Halldorson JB, Bakthavatsalam R, Fix OK, Carithers RL, Jr., Reyes JD. Should liver transplantation in patients with model for end-stage liver disease scores ≤14 be avoided? A decision analysis approach. Liver Transpl 2009;15:242-254.
5) Volk ML, Hernandez JC, Lok AS, Marrero JA. Modified Charlson comorbidity index for predicting survival after liver transplantation. Liver Transpl 2007;13:1515-1520.
6) Lipshutz GS, Busuttil RW. Liver transplantation in those of advancing age: the case for transplantation. Liver Transpl 2007;13: 1355-1357.
7) Strom SC, Chowdhury JR, Fox IJ. Hepatocyte transplantation for the treatment of human disease. Semin Liver Dis 1999;19:39-48.
8) Rhim JA, Sandgren EP, Degen JL, Palmiter RD, Brinster RL. Replacement of diseased mouse liver by hepatic cell transplantation. Science 1994;263:1149-1152.
9) Weglarz TC, Degen JL, Sandgren EP. Hepatocyte transplantation into diseased mouse liver. Kinetics of parenchymal repopulation and identification of the proliferative capacity of tetraploid and octaploid hepatocytes. Am J Pathol 2000;157:1963-1974.
10) Braun KM, Sandgren EP. Cellular origin of regenerating parenchyma in a mouse model of severe hepatic injury. Am J Pathol 2000;157:561-569.
11) Grompe M, Lindstedt S, Al-Dhalimy M, Kennaway NG, Papaconstantinou J, Torres-Ramos CA, et al. Pharmacological correction of neonatal lethal hepatic dysfunction in a murine model of hereditary tyrosinaemia type I. Nat Genet 1995;10:453-460.
12) Overturf K, al-Dhalimy M, Ou CN, Finegold M, Grompe M. Serial transplantation reveals the stem-cell-like regenerative potential of adult mouse hepatocytes. Am J Pathol 1997;151:1273-1280.
13) Lagasse E, Connors H, Al-Dhalimy M, Reitsma M, Dohse M, Osborne L, et al. Purified hematopoietic stem cells can differentiate into hepatocytes in vivo. Nat Med 2000;6:1229-1234.
14) Grompe M. Principles of therapeutic liver repopulation. J Inherit Metab Dis 2006;29:421-425.
15) Grompe M, Overturf K, al-Dhalimy M, Finegold M. Therapeutic trials in the murine model of hereditary tyrosinaemia type I: a progress report. J Inherit Metab Dis 1998;21:518-531.
16) Overturf K, Al-Dhalimy M, Tanguay R, Brantly M, Ou CN, Finegold M, et al. Hepatocytes corrected by gene therapy are selected in vivo in a murine model of hereditary tyrosinaemia type I. Nat Genet 1996;12:266-273.
17) Elgilani F, Mao SA, Glorioso JM, Yin M, Iankov ID, Singh A, et al. Chronic phenotype characterization of a large-animal model of hereditary tyrosinemia type 1. Am J Pathol 2017;187:33-41.
18) Hickey RD, Mao SA, Glorioso J, Elgilani F, Amiot B, Chen H, et al. Curative ex vivo liver-directed gene therapy in a pig model of hereditary tyrosinemia type 1. Sci Transl Med 2016;8:349ra99.
19) Hickey RD, Mao SA, Glorioso J, Lillegard JB, Fisher JE, Amiot B, et al. Fumarylacetoacetate hydrolase deficient pigs are a novel large animal model of metabolic liver disease. Stem Cell Res 2014;13:144-153.
20) Fox IJ, Chowdhury JR, Kaufman SS, Goertzen TC, Chowdhury NR, Warkentin PI, et al. Treatment of the Crigler-Najjar syndrome type I with hepatocyte transplantation. N Engl J Med 1998;338:1422-1426.
21) Nishikawa T, Bell A, Brooks JM, Setoyama K, Melis M, Han B, et al. Resetting the transcription factor network reverses terminal chronic hepatic failure. J Clin Invest 2015;125:1533-1544.
22) Komori J, Boone L, DeWard A, Hoppo T, Lagasse E. The mouse lymph node as an ectopic transplantation site for multiple tissues. Nat Biotechnol 2012;30:976-983.
23) Hoppo T, Komori J, Manohar R, Stolz DB, Lagasse E. Rescue of lethal hepatic failure by hepatized lymph nodes in mice. Gastroenterology 2011;140:656-666.
24) Gramignoli R, Green ML, Tahan V, Dorko K, Skvorak KJ, Marongiu F, et al. Development and application of purified tissue dissociation enzyme mixtures for human hepatocyte isolation. Cell Transplant 2012;21:1245-1260.
25) Starzl TE, Porter KA, Francavilla A. The Eck fistula in animals and humans. Curr Probl Surg 1983;20:687-752.
26) Starzl TE, Watanabe K, Porter KA, Putnam CW. Effects of insulin, glucagon, and insuling/glucagon infusions on liver morphology and cell division after complete portacaval shunt in dogs. Lancet 1976;1:821-825.
27) Michalopoulos GK. Hepatostat: liver regeneration and normal liver tissue maintenance. Hepatology 2017;65:1384-1392.
28) Deng X, Zhang X, Li W, Feng RX, Li L, Yi GR, et al. Chronic liver injury induces conversion of biliary epithelial cells into hepatocytes. Cell Stem Cell 2018;23:114-122.
29) Schaub JR, Huppert KA, Kurial SNT, Hsu BY, Cast AE, Donnelly B, et al. De novo formation of the biliary system by TGFβ-mediated hepatocyte transdifferentiation. Nature 2018;557:247-251.
30) Hussein A, Wyatt J, Guthrie A, Stringer MD. Kasai portoenterostomy—new insights from hepatic morphology. J Pediatr Surg 2005;40:322-326.
31) Beckett GJ, Percy-Robb IW. Bile salt transport in intestinal lymph of the rat. Eur J Clin Invest 1982;12:23-27.
32) Ewerth S. On the enterohepatic circulation of bile acids in man. Acta Chir Scand Suppl 1982;513:1-38.
33) Ewerth S, Björkhem I, Einarsson K, Ost L. Lymphatic transport of bile acids in man. J Lipid Res 1982;23:1183-1186.
34) Kohan A, Yoder S, Tso P. Lymphatics in intestinal transport of nutrients and gastrointestinal hormones. Ann N Y Acad Sci 2010;1207(suppl 1):E44-E51.
35) Rastogi A, Maiwall R, Bihari C, Trehanpati N, Pamecha V, Sarin SK. Two-tier regenerative response in liver failure in humans. Virchows Arch 2014;464:565-573.
36) Pravisani R, Soyama A, Ono S, Baccarani U, Isola M, Takatsuki M, et al. Is there any correlation between liver graft regeneration and recipient's pretransplant skeletal muscle mass? a study in extended left lobe graft living-donor liver transplantation. Hepatobiliary Surg Nutr 2020;9:183-194.
37) Schawkat K, Reiner CS. Diffuse liver disease: cirrhosis, focal lesions in cirrhosis, and vascular liver disease. In: Hodler J, Kubik-Huch RA, von Schulthess GK, eds. Diseases of the Abdomen and Pelvis 2018-2021: Diagnostic Imaging - IDKD Book. Cham, Switzerland: Springer; 2018:229-236.
38) Soltys KA, Setoyama K, Tafaleng EN, Soto Gutiérrez A, Fong J, Fukumitsu K, et al. Host conditioning and rejection monitoring in hepatocyte transplantation in humans. J Hepatol 2017;66:987-1000.
39) Fletcher AL, Malhotra D, Turley SJ. Lymph node stroma broaden the peripheral tolerance paradigm. Trends Immunol 2011;32:12-18.